The TGO formation in overaluminized TBC obtained using plasma spray physical vapour deposition process during cyclic and isothermal oxidation

M. Góral[1]*, T. Kubaszek[1], R. Swadzba[2], M. Pytel[1]

[1] *Research and Development Laboratory for Aerospace Materials, Rzeszow University of Technology, Powstancow Warszawy 12, 35-959 Rzeszow, Poland*
[2] *Stanisław Staszic Institute for Ferrous Metallurgy, K. Miarki 12-14, 44-100 Gliwice, Poland*

Abstract

The article presents the results of the microstructural characterization of the newly developed three-layer thermal barrier coating after isothermal oxidation tests. Bond coats were produced by the CVD-overaluminizing of previously low-pressure plasma sprayed (LPPS) MCrAlY coating. The outer ceramic layer was produced by the plasma spray physical vapour deposition method (PS-PVD). For comparison, the MCrAlY bond coat without aluminizing was produced by LPPS. As a result of the overaluminizing process, the formation of the NiAl aluminide layer was observed. Also, the porosity was observed as a result of the Kirkendall effect in the middle zone of the bond coat. Three-layer TBCs microscopic examination showed the formation of a thin and dense TGO layer formed from alumina oxide. The porosity observed on as-deposited three-layer TBCs disappeared during the cyclic oxidation test. A thicker and delaminated TGO layer was formed in a conventional two-layered thermal barrier coating. The isothermal oxidation test at 1100 ℃ for 1000 h shows that TGO (Thermally Grown Oxides) alumina oxide layer on the overaluminized bond coat was also significantly thinner compared to conventional LPPS-sprayed MCrAlY bond coats. It was concluded that the formation of the TGO layer in three-layer TBC is similar to that observed in diffusion aluminide coatings. The overaluminizing can improve the oxidation resistance of thermal barrier coatings produced by LPPS and PS-PVD methods.

K e y   w o r d s: thermal barrier coatings (TBC), aluminide coating, plasma spraying, low-pressure plasma spraying (LPPS), plasma spray physical vapour deposition (PS-PVD), oxidation, thermally grown oxides (TGO)

1. Introduction

Increasing the temperatures in the hot turbine section requires the use of advanced materials, such as single-crystal nickel-base superalloys but also protective coatings [1]. Current research is focused on developing more efficient coatings, which protect the blade surface from high temperatures and corrosion [2]. Thermal barrier coating (TBC) is widely used in industrial environments, whose individual layers play different roles [3]. The MCrAlY type inner metallic bond coat protects the surface of material against corrosive agents, while the outer ceramic layer is a thermal insulator [4, 5]. For first-stage turbine blades, a diffusion aluminide coating-based modified by platinum, hafnium, palladium and zirconium addition is used. The ceramic layer with lower thickness and roughness is formed by EB-PVD – electron beam physical vapour deposition [6, 7]. Aluminide diffusion coatings, which mainly contain β-NiAl phase, are used as bond coats for ceramic layers deposited by the EB-PVD method. They are produced by pack cementation, out-of-pack, and chemical vapour deposition (CVD) [8–10]. The oxidation resistance of the MCrAlY bond coats can be improved by the overaluminizing process and the formation of a pure NiAl

Table 1. The results of the chemical composition analysis in the areas marked in Fig. 1

Area	Element content (at.%)						
	Zr	Y	O^s	Al	Cr	Co	Ni
1	29.4	4.7	65.9	–	–	–	–
2	–	–	–	11.3	25.6	26.9	36.2
3	–	–	–	37.9	5.4	10.6	46.1
4	25.5	3.2	64.1	–	2.4	1.9	2.9
5	–	–	55.9	13.2	10.5	7.9	12.5

^{s} – stochiometric

phase on its surface [11, 12]. New technology of production of a columnar ceramic layer in thermal barrier coatings called Plasma Spray Physical Vapour Deposition (PS-PVD) was developed [13]. The concept of an overaluminized MCrAlY layer was developed as a bond coat for that type of ceramic layer. In three-layer TBCs, the MCrAlY bond coat was sprayed by a low-pressure plasma spraying method (LPPS) and aluminized by the CVD process. The ceramic coating with a columnar structure was deposited using the newly developed PS-PVD process [14]. Previous work practices have shown that the type of base material does not affect the formation of TGO in an isothermal oxidation test [15, 16]. The article presents the microstructural characteristics of the obtained coating on the nickel superalloy IN 713 and the formation of the TGO layer in cyclic and isothermal oxidation tests.

2. Experimental

Samples made from Inconel 713-nickel superalloy with a diameter of 20 mm and a thickness of 4 mm were washed and sandblasted with electrocorundum before coatings were produced. Bond coats were produced using the LPPS Hybrid system (Oerlikon-Metco) and commercial Amdry 386 (Oerlikon-Metco) powder with a nominal chemical composition (in wt.%): Co: 19–26, Cr: 14–21, Al: 11–14, Hf: 0.1–0.5, Y: 0.2–0.8, Si: 0.1–0.7, Ni: bal. Half of the samples with MCrAlY bond coats were additionally overaluminized in the low-activity CVD process. The aluminizing process was conducted using the Bernex BPX Pro 325S (IonBond) system, configuration parameters included in the paper [17]. Plasma spraying of the ceramic coating was carried out by the PS-PVD method using the LPPS – Hybrid system (Oerlikon Metco). Specifically designed powder for the PS-PVD process (Metco 6700) for yttria-stabilized zirconia (YSZ) was used for the production of TBC. The oxidation test was conducted in 23-hour heating at 1100 ℃ and 1-hour cooling in one cycle in static laboratory air. The microstructural survey was conducted after 35 oxidation cycles. Isothermal oxidation resistance tests were car-
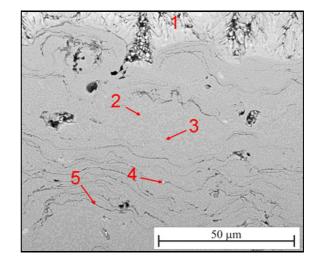

Fig. 1. The microstructure of as-deposited two-layer thermal barrier coating with marked areas of chemical composition analysis.

ried out at the temperature of 1100 ℃ in static laboratory air for 1000 h. Cylindrical shaped samples placed on aluminium oxide bed were used. Cross-sections of the samples were prepared, and then the coatings were analysed using a Scanning Electron Microscope (SEM) type Hitachi S-3400 and FEI Inspect F.

3. Results and discussion

3.1. The microstructure of as-deposited two-layer TBC

The thermal barrier coating obtained by low-pressure plasma spraying of the bond coat and deposition of the ceramic coating by the PS-PVD method had a typical two-layer structure. The MCrAlY type bond coat had an average thickness of 80 μm, and the outer column ceramic layer was approximately 100 μm thick. In the outer ceramic layer (area 1 in Fig. 1, Table 1) the presence of zirconium, yttrium and oxygen – the elements forming YSZ –was detected. Chemical composition analysis in the bond coating showed the presence of high-aluminium content precipitations

T a b l e 2. The results of the chemical composition analysis in the areas marked in Fig. 2

Area	Element content (at.%)									
	Zr	Y	O^s	Al	Cr	Co	Ni	Mo	Nb	Ti
1	30.2	3.8	66.0	–	–	–	–	–	–	–
2	–	–	–	44.8	2.8	11.8	40.6	–	–	–
3	–	–	57.3	27.2	2.1	3.4	10.0	–	–	–
4	–	–	36.7	–	7.5	13.4	42.0	0.4	–	–
5	–	–	–	2.2	86.1	5.5	5.6	0.6	–	–
6	–	–	–	28.5	18.8	17.5	34.6	0.6	–	–
7	–	–	–	26.8	13.9	15.6	43.7	–	–	–
8	–	–	–	16.9	22.1	20.0	40.1	0.9	–	–
9	–	–	–	9.6	26.9	20.5	41.3	1.2	0.5	–
10	–	–	–	35.9	6.7	8.7	48.7	–	–	–
11	–	–	–	13.6	13.2	–	69.1	2.0	0.9	1.2

^{s} – stochiometric

(area 3 in Fig. 1) – possible β-NiAl grains typical for MCrAlY bond coat. Besides, grains with the low Al were also detected (area 2 in Fig. 1, Table 1). The presence of multi-component oxides in the pores that formed during the plasma spraying process was also noted (area 4, 5 in Fig. 1, Table 1).

The three-layer thermal barrier coating with additional low-activity aluminized MCrAlY bond coat was characterized by a multilayer structure (Fig. 2). The analysis of the chemical composition of the outer ceramic layer confirmed the presence of Zr, Y, and O forming the YSZ columns (Fig. 2a, area 1, Table 2). In the outer zone of the bond coat (area 2 in Fig. 2a), the concentration of Ni (40.6 at.%) and Al (44.8 at.%) shows the formation of layers of NiAl crystals with a thickness 10–15 µm. Below this layer (area 3 in Fig. 2a) a high concentration of aluminium and oxygen suggests the formation of a thin alumina--oxide layer. In area 4 (Fig. 2a), the presence of Ni and O was detected. In the middle zone of the bond coat, some porosity was observed as a result of the Kirkendall effect (Fig. 2a). High chromium concentration in area 5 was detected (Fig. 2a). In area 6, the concentration of Al was lower (28.5 at.%) than that in the outer overaluminized zone of the bond coat (about 45 at.% in area 2). Precipitations with lower Al, higher Co and Cr content were detected in the inner zone (area 8 in Fig. 2b). In the matrix (area 7 in Fig. 2b) of this zone, a higher Al content suggests the formation of low Al phases from the Ni-Al system (probably Ni$_3$Al). Lower aluminium content and higher Co and Cr concentration were observed at the interface of the bond coat/base material. A high concentration of Al and Ni in precipitation marked "10" in Fig. 10 allows the formation of NiAl phase crystals to be completed. In area 11 (Fig. 10), the concentration of elements was similar to the nominal composition of the Inconel 713 superalloy.

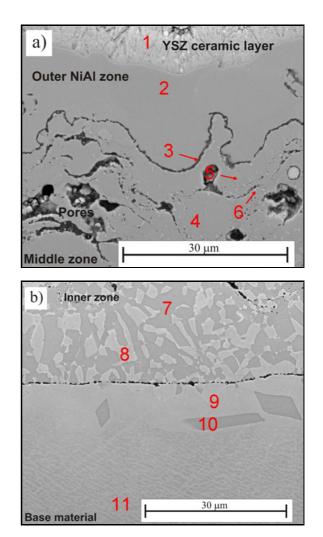An elementary map of the cross-section of the ob-

Fig. 2. The microstructure of three-layer TBC: (a) outer and (b) inner zone of overaluminized bond coat with marked areas of chemical composition analysis.

tained three-layer thermal barrier coatings (Fig. 3) confirmed the results of the chemical composition
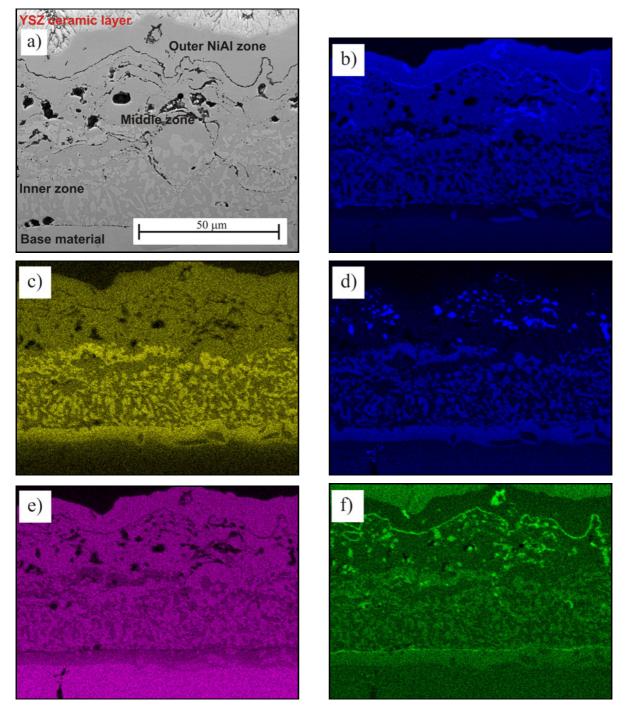
Fig. 3. Microstructure (a) and elemental map: Al (b), Co (c), Cr (d), Ni (d), O (e), and Zr (g) of the cross-section of an as-deposited three-layer thermal barrier coating.

analysis in the micro areas. A high concentration of Zr (Fig. 3g) with the presence of O (Fig. 3f) was observed in the outer columnar ceramic layer. Also, a high concentration of O and Al was observed (Fig. 3b) in a thin layer between the outer and middle zone of the metallic bond coat. This suggests the formation of a thin layer of alumina oxide. A similar thin layer of alumina could be formed on the interface of bond coat/base material. The presence of Ni (Fig. 3e) and

Al was observed in the outer zone of the bond coat. A higher concentration of Co (Fig. 3c) and Cr (Fig. 3d) was also observed in precipitations in the middle and outer zone of the bond coat.

3.2. TBC microstructure after cyclic oxidation test

The oxidation test of obtained TBCs at 1100 °C

Table 3. The results of the chemical composition analysis in the areas marked in Fig. 4

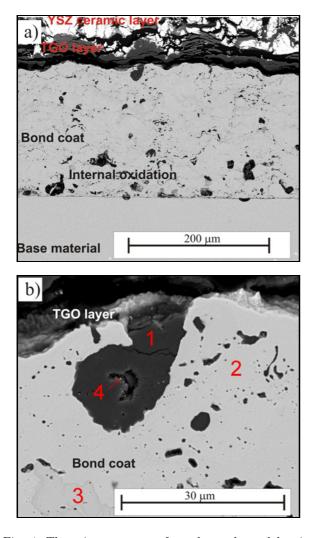| Area	Element content (at.%)						
	O^s	Al	Cr	Co	Ni	Mo	Nb
1	60.0	40.0	–	–	–	–	–
2	–	14.6	15.9	10.9	56.6	1.2	0.8
3	–	33.6	5.6	6.1	54.7	–	–
4	58.6	30.2	4.4	2.5	4.3	–	–

^{s} – stochiometric

Fig. 4. The microstructure of two-layer thermal barrier coating after cyclic oxidation testing (a) and its TGO layer with marked areas of chemical composition analysis (b).
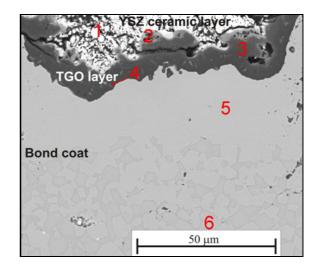
Fig. 5. The microstructure of a three-layer thermal barrier coating after cyclic oxidation testing with the marked areas of chemical composition analysis.

was completed after 35 cycles for microscopic assessment. The presence of a thick and delaminated TGO layer was observed in a conventional two-layer thermal barrier coating (Fig. 4a). The effects of internal oxidation were also visible throughout the entire bond coat. The results of the analysis of the chemical composition of the TGO layer (areas 1 and 4 in Fig. 4b, Table 3) showed that the aluminium and oxygen are

their main components. Measured concentrations of these elements may suggest the formation of almost pure aluminium oxide in the TGO layer. A reduction in the Al concentration in the bond coat near the TGO layer was observed (area 2, Fig 4b). In area 3 (Fig. 4b) the higher content of Al (33.6 at.%, Table 3) and Ni (56.7 at.%, Table 3) may be due to the presence of the NiAl phase (formed during plasma spraying) or the Ni_3Al phase (formed during outward Al diffusion and forming the TGO layer).

A thick, dense TGO layer formed in the three-layer thermal barrier coating during the cyclic oxidation test. The presence of the main elements (Zr, Y, O) of stabilized yttria zirconia was detected in the outer ceramic layer (Fig. 5, area 1, Table 4). Analysis of the chemical composition in area 2 (Fig. 5, Table 4) showed a high concentration of aluminium and oxygen, as well as the presence of Cr, Co, Ni. Only aluminium and oxygen were detected in other TGO analysed areas. It can be stated that pure aluminium oxide forms a TGO layer during cyclic oxidation. Microscopic examination showed that during the cyclic oxidation test, the porosity observed in the as-deposited overaluminized bond coat disappeared. In the outer zone of the bond coat, below TGO alloy, a

Table 4. The results of the chemical composition analysis in the areas marked in Fig. 5

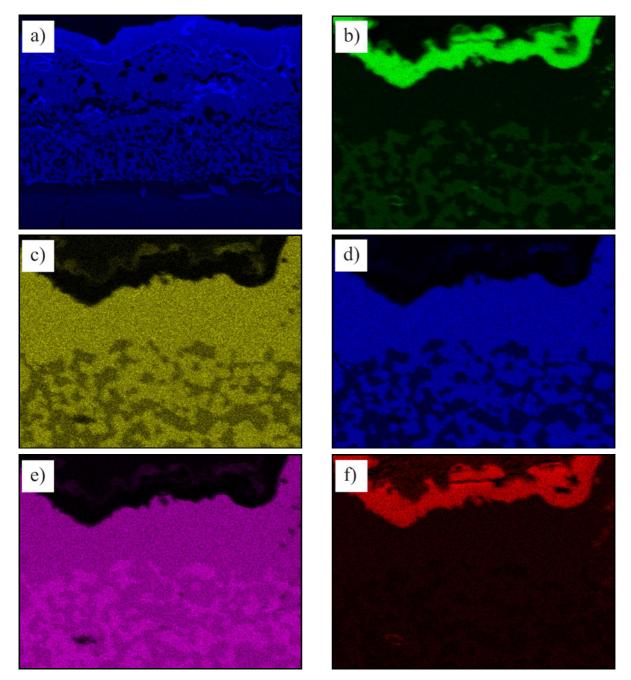| Area	Element content (at.%)						
	Zr	Y	O^s	Al	Cr	Co	Ni
1	30.2	3.7	66.1	–	–	–	–
2	0.5	–	57.9	25.4	5.7	5.2	5.3
3	–	–	60.0	40.0	–	–	–
4	–	3.9	60.0	36.1	–	–	–
5	–	–	–	12.9	20.6	21.7	44.8
6	–	–	–	34.0	6.2	10.6	49.2
7	–	–	–	13.4	19.9	21.4	45.3

^{s} – stochiometric

Fig. 6. Elemental map: Zr (a), Al (b), Co (C), Cr (d), Ni (d), and O (f) from the cross-section of a three-layer thermal barrier coating after the cyclic oxidation test presented/shown in Fig. 5.

Table 5. The results of the chemical composition analysis in the areas marked in Fig. 7

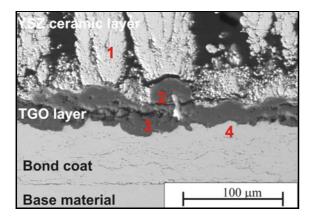| Area	Element content (at.%)									
	Mo	O^s	Al	Cr	Co	Ni	Y	Zr	Ti	Hf
1	–	65.3	1.2	0.4	0.5	2.0	2.4	27.7	0.3	0.3
2	–	59.0	26.2	1.1	4.0	7.0	0.6	1.4	0.7	–
3	–	59.9	37.5	0.2	0.3	1.1	0.2	0.6	0.2	–
4	1.0	–	8.4	19.0	12.5	57.9	0.2	0.9	–	0.1

^{s} – stochiometric

Fig. 7. The microstructure of the two-layer thermal barrier coating after the isothermal oxidation test with the marked areas of chemical composition analysis.
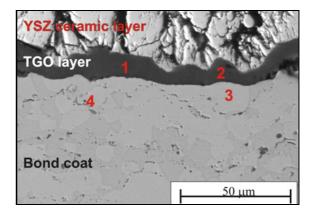

Fig. 8. The microstructure of the three-layer thermal barrier coating after the isothermal oxidation test with the marked areas of chemical composition analysis.

reduction in Al content was detected (area 5, Fig. 5, Table 4). This was a consequence of outward diffusion of Al and the formation of the TGO layer. A higher concentration of aluminium was found in the inner zone of the bond coat (area 6, Fig. 5, Table 4). The content of Al and Ni at this point may suggest the presence of a NiAl or Ni$_3$Al phase. In area 7 (Fig. 5, Table 4), the Al concentration was significantly lower and did not exceed 15 at.%.

The elemental mapping of three-layer TBCs after the cyclic oxidation test is presented in Fig. 6. It has been shown that Zr concentration dominates in the outer ceramic layer (Fig. 6a). Below, the high concentration of aluminium (Fig. 6b) and oxygen (Fig. 6f) confirms the formation of the TGO Al$_2$O$_3$ layer during the cyclic oxidation test. Co- (Fig. 6c) and Cr-rich (Fig. 6d) precipitation with Ni-content was detected in the bond coat. Higher Al concentration was observed in the matrix area between these participations (Fig. 6b).

3.3. Microstructure after the isothermal oxidation test

In a conventional two-layer thermal barrier coating, a thick TGO layer with cracks formed during the isothermal oxidation test. No effects of internal oxida-

tion of the bond coat were observed (Fig. 7). Analysis of the chemical composition in the outer ceramic layer (area 1 in Fig. 7, Table 5) showed the content of oxygen, zirconium, and yttrium, which form YSZ. The presence of other elements such as Cr, Al, Ni, Ti, and Hf was also detected. In the TGO layer (areas 2, 3 in Fig. 7), Al and O were the main components. The presence of Ni, Co, Cr, and Zr in the TGO layer in area 2 (Fig. 7) may be a consequence of the formation not only Al$_2$O$_3$ but also other oxides and spinels.

Microscopic observation of the three-layer thermal barrier coating after a 1000-hour isothermal oxidation test showed the disappearance of the porosity formed in the as-deposited bond coat. Analysis of the chemical composition of the TGO layer (area 1, 2, Fig. 8) formed during isothermal oxidation showed the presence of only Al and O. It can be stated that alumina oxide is a main component of the TGO layer. High concentrations of Al (32.6 at.%) and Ni (almost 60 at.%) in the outer area of the bond coat (area 3, Fig. 8, Table 6) may be due to the presence of the NiAl phase. Higher Cr content and lower Al content were observed in area 4 (Fig. 8).

4. Conclusions

The concept of additional aluminizing of a con-

T a b l e 6. The results of the chemical composition analysis in the areas marked in Fig. 8

Area	Element content (at.%)								
	O^s	Al	Cr	Co	Ni	Y	Zr	Ti	Mo
1	59.9	38.0	0.3	–	1.1	0.1	0.6	–	–
2	59.9	37.8	0.3	–	1.1	0.1	0.7	–	–
3	–	32.6	6.7	–	59.3	–	0.9	0.3	0.1
4	–	16.1	18.8	–	62.8	–	0.9	0.2	1.2

^{s} – stochiometric

ventional two-layer thermal barrier coating with an MCrAlY bond coat was investigated. A mechanism for forming a bond coat during the low-activity aluminizing process has been described. It was found that during the aluminizing process, a layer of NiAl aluminide with thickness 15–20 μm was formed [18]. Below, a very thin (< 1 μm) layer of alumina oxide was probably formed during the plasma spraying process. A large number of pores were observed in the middle area of the bond-coat. The reference [19] suggests their formation as a result of the Kirkendall effect. Two types of precipitation with varying concentrations of Al were detected in the inner zone of the bond coat. It can be concluded that precipitations with a higher aluminium content form a NiAl or Ni_3Al phase. Also, the elemental mapping of the overaluminized bond coat layer showed the possibility of the presence of a very thin alumina layer in the interface of the bond coat/base material. In the conventional MCrAlY bond coat, the β-NiAl and γ-Ni phases are the main constituents.

During the cyclic oxidation test of a conventional two-layer thermal barrier coating, a thick TGO layer with cracks and delamination was formed. The effects of the internal oxidation of the bond coat have also been observed [20]. A thin and dense TGO layer was formed in the newly developed three-layer TBC. The results of the chemical composition analysis show that the TGO layer is formed from almost pure Al_2O_3 oxide, which increases the oxidation resistance of the developed three-layer TBC [21]. Besides, previously observed pores disappeared during the oxidation process. Al depletion was detected by its outward/external diffusion from the bond coat and the formation of alumina oxide. Based on the results of the chemical composition analysis, the presence of high-Al contains precipitates – a NiAl phase could probably occur deeper in the bond coat.

After 1000 h of isothermal oxidation test, no internal oxidation effects in two-layer TBC were observed. A thick TGO layer with a large number of cracks formed in the interface ceramic layer/bond layer. The presence of elements other than Al and O suggests the formation of other oxides and spinels in the TGO layer formed in the two-layer TBC during isothermal oxidation [21–23]. The porosity and thermal expansion

coefficient in double-layer TBC can play an important role in its degradation [24]. Additionally, the MCrAlY contains two-phases: β-NiAl and γ-Ni solid solution. As a consequence, the Al reservoir is smaller than that in a single NiAl zone in three-layer TBC, and the formation of TGO is more rapidly. The thin and dense TGO layer was formed during isothermal oxidation of three-layer thermal barrier coating. Probably, the formation mechanism of the TGO layer in three-layer TBC is similar to that observed in diffusion aluminide coatings [11]. The alumina oxide is formed in this condition [25]. Based on the results of the chemical composition analysis, it can be concluded that alumina oxide is the main phase in these TGO layers.

The results of the conducted research showed that newly developed three-layer TBCs produced using advanced plasma spraying processes (LPPS and PS-PVD) can improve the corrosion resistance of turbine blades. The additional of overaluminizing process allows the formation of thin alumina oxide under isothermal and cyclic oxidation conditions.

Acknowledgements

References

[1] R. A. Miller, Thermal barrier coatings for aircraft engines: History and directions, Journal of Thermal Spray Technol. 6 (1997) 35–42. doi:10.1007/BF02646310

[2] M. J. Pomeroy, Coatings for gas turbine materials and long term stability issues, Mater. and Design 26 (2005) 223–231. doi:10.1016/j.matdes.2004.02.005

[3] G. W. Goward, Progress in coatings for gas turbine airfoils, Surf. and Coat. Technol. 108–109 (1998) 73–79. doi:10.1016/S0257-8972(98)00667-7

[4] M. Goral, S. Kotowski, K. Dychton, M. Drajewicz, T. Kubaszek, Influence of low pressure plasma spraying parameters on MCrAlY bond coat and its microstructure, Key Eng. Mat. 592–593 (2013) 421–424. doi:10.4028/www.scientific.net/KEM.592-593.421

[5] D. M. Comassar, Surface coatings technology for turbine engine applications, Metal Finishing 89 (1991) 39–44.

[6] A. Matthews, S. J. Young, M. Joseph, C. Rebholz, J. M. Schneider, S. J. Dowey, Partially yttria-stabilized zirconia coatings produced under plasma-assisted EBPVD with bipolar pulsed bias and under electron bombardment-assisted positive bias conditions, Surf. and Coat. Technol. 94–95 (1997) 123–130. doi:10.1016/S0257-8972(97)00489-1

[7] Y. H. Sohn, R. R. Biederman, R. D. Sisson Jr., Microstructural development in physical vapour-deposited partially stabilized zirconia thermal barrier coatings, Thin Sol. Films 250 (1994) 1–7. doi:10.1016/0040-6090(94)90155-4

[8] G. W. Goward, D. H. Boone, Mechanisms of formation of diffusion aluminide coatings on nickel--base superalloys, Oxid. of Met. 3 (1971) 475–495. doi:10.1007/BF00604047

[9] A. Squillace, R. Bonetti, N. J. Archer, J. A. Yeatman, The control of the composition and structure of aluminide layers formed by vapour aluminising, Surf. and Coat. Technol. 120–121 (1999) 118–123. doi:10.1016/S0257-8972(99)00347-3

[10] M. Warnes, Reactive element modified chemical vapor deposition low activity platinum aluminide coatings, Surf. and Coat. Technol. 146–147 (1997) 7–12. doi:10.1016/S0257-8972(01)01363-9

[11] B. M. Warnes, Improved aluminide/MCrAlX coating systems for super alloys using CVD low activity aluminizing, Surf and Coat. Technol. 163–164 (2003) 106–111. doi:10.1016/S0257-8972(02)00602-3

[12] M. Goral, S. Dudek, S. Filip, J. Sieniawski, Microstructure of thermal barrier coatings (TBCs) obtained by using plasma spraying and VPA methods, Mat. Sci. Forum 706–709 (2012) 2412–2417. doi:10.4028/www.scientific.net/MSF.706-709.2412

[13] M. Góral, J. Sieniawski, S. Kotowski, M. Pytel, M. Masłyk, Influence of turbine blade geometry on thickness of TBCs deposited by VPA and PS-PVD methods, Arch. of Mat. Sci. and Eng. 54 (2012) 22–28.

[14] M. Goral, M. Pytel, M. Drajewicz, The formation of TBCs using LPPS, CVD and PS-PVD methods on CMSX-4 single-crystal nickel superalloy, Sol. St. Phen. 227 (2015) 317–320. doi:10.4028/www.scientific.net/SSP.227.317

[15] M. Goral, M. Pytel, W. Cmela, M. Drajewicz, The influence of overaluminizing on TGO formation on thermal barrier coatings deposited by low pressure plasma spraying and chemical vapour deposition methods on Rene 80 nickel superalloy, Sol. St. Phen. 227 (2015) 321–324. doi:10.4028/www.scientific.net/SSP.227.321

[16] M. Góral, The influence of overaluminizing on TGO formation on CMSX-4 nickel superalloy during isothermal oxidation, Mat. Sci. For. 844 (2016) 193–196. doi:10.4028/www.scientific.net/MSF.844.193

[17] A. Nowotnik, M. Goral, M. Pytel, K. Dychton, Influence of coatings deposition parameters on microstructure of aluminide coatings deposited by CVD method on Ni-superalloys, Sol. St. Phen. 197 (2013) 95–100. doi:10.4028/www.scientific.net/SSP.197.95

[18] P. Ch. Tsai, Ch. F. Tseng, Ch.-W. Yang, I.-Ch. Kuo, Y.-L. Chou, J. W. Lee, Thermal cyclic oxidation performance of plasma sprayed zirconia thermal barrier coatings with modified high velocity oxygen fuel sprayed bond coatings, Surf. and Coat. Technol. 228 (2013) S11–S14. doi:10.1016/j.surfcoat.2012.10.004

[19] M. Mohammadi, S. A. J. Jahromi, S. Javadpour, A. Kobayashi, K. Shirvani, Hot corrosion behavior and microstructural change of Al-gradient CoNiCrAlYSi coatings, produced by LVPS and diffusional processes, Oxid. Met. 78 (2012) 17–30. doi:10.1007/s11085-012-9288-4

[20] A. Jalowicka, D. Naumenko, M. Ernsberger, R. Herzog, W. J. Quadakkers, Alumina formation and microstructural changes of aluminized CoNiCrAlY coating during high temperature exposure in the temperature range 925 °C–1075 °C, Mat. at High Temp. 35 (2018) 66–77. doi:10.1080/09603409.2017.1392114

[21] M. Tahari, F. Naeimi, Effect of surface morphologies on the isothermal oxidation behavior of MCrAlY coatings fabricated by high-velocity oxyfuel processes, IJE Transactions C 30 (2017) 433–439. doi:10.5829/idosi.ije.2017.30.03c.13

[22] B.-Y. Zhang, G.-J. Yang, Ch.-X. Li, Ch.-J. Li, Non--parabolic isothermal oxidation kinetics of low pressure plasma sprayed MCrAlY bond coat, Appl. Surf. Sci. 406 (2017) 99–109. doi:10.1016/j.apsusc.2017.02.123

[23] W. R. Chen, X. Wu, B. R. Marple, P. C. Patnaik, The growth and influence of thermally grown oxide in a thermal barrier coating, Surf and Coat. Technol. 201 (2006) 1074–1079. doi:10.1016/j.surfcoat.2006.01.023

[24] X. Li, X.-Y. Peng, H. Dong, Y. Zhou, T. Wang, K. Ren, S. Liang, The evaluation of durability of plasma-sprayed Thermal Barrier Coatings with double-layer bond coat, Coatings 9 (2019) 433–439. doi:10.3390/coatings9040241

[25] R. Swadzba, L. Swadzba, J. Wiedermann, M. Hetmanczyk, B. Witala, Characterization of alumina scales grown on a 2nd generation single crystal Ni superalloy during isothermal oxidation at 1050, 1100 and 1150 °C, Oxid. Met. 86 (2014) 195–208. doi:10.1007/s11085-014-9487-2